Interference effects in high-order harmonic generation with molecules

M. Lein, N. Hay, R. Velotta,* J. P. Marangos, and P. L. Knight
Blackett Laboratory, Imperial College of Science, Technology and Medicine, London SW7 2BW, United Kingdom
(Received 24 April 2002; published 6 August 2002)

We study high-order harmonic generation for H_2^+ and H_2 model molecules in linearly polarized laser pulses by numerical solution of the Schrödinger equation. Maxima and minima due to intramolecular interference are found in the dependence of the harmonic intensities on the internuclear distance and on the orientation of the molecules. These extrema can be approximately predicted by regarding them as the result of interference between two radiating point sources located at the positions of the nuclei.

DOI: 10.1103/PhysRevA.66.023805 PACS number(s): 42.65.Ky, 33.80.Rv

When matter is subject to intense laser irradiation, high-order harmonics are generated [1–4] as a consequence of the highly nonlinear dynamics. Atoms and molecules behave similarly as far as the broad features of this process are concerned. In both cases, the harmonic spectra contain a nonperturbative plateau with a cutoff at a photon energy which is predicted by a simple recollision model [5,6]. This model assumes that a harmonic photon is generated by the recollision of an electron with the core after the electron was ejected by tunnel ionization and driven back by the laser field. Effects which are specific to small molecules are not easily observed experimentally because experiments are usually performed with randomly oriented molecules. This seems to be the reason why many details of theoretical predictions [7–15] have not yet been confirmed experimentally. To study details depending on the molecular structure and orientation, molecules should be prealigned prior to the actual process of harmonic generation. Such alignment was demonstrated in recent experiments [16,17] where a combination of an aligning picosecond pulse and an intense femtosecond pump pulse was used. We expect that this technique will open the way for a much more detailed investigation of high-order harmonic generation (HHG) in molecules.

Previous theoretical work [9,11,12,18] showed that HHG with linearly polarized laser pulses is sensitive to the molecular orientation. In particular, we recently found [18] that the intensity of a harmonic is minimized when the orientation of the molecule relative to the field is at a ''critical angle.'' The phase of the harmonic is almost constant except at the critical angle where it undergoes a jump by about π radians. These effects were shown to arise from intramolecular interference and are further investigated in the present paper. We show that not only minima but also maxima are found in the orientation dependence of the harmonic yield. Further, the same effects are found when the internuclear distance is varied while the orientation of the molecule is fixed. We show that the positions of the interference extrema are approximately reproduced by simple formulas, suggesting an analogy to the interference between two point sources. The harmonic spectra thus carry structural information about the molecules. These effects may be closely related to ''dynamic electron diffraction'': Interference patterns are also expected in the angular distribution of photoelectrons that are scattered from the molecular core [19]. For diatomic molecules, both phenomena may be viewed as microscopic two-slit experiments.

To investigate the orientation dependence of HHG, we employ two-dimensional (2D) models of the H_2^+ and H_2 molecules where the nuclei are fixed and the electronic motion is restricted to the plane spanned by the molecular axis and the laser polarization axis. The H_2 molecule is treated within the Hartree-Fock approximation, i.e., the calculation involves the propagation of a single-electron wave function as in the case of H_2^+. The difference is that the potential seen by the electron contains an additional mean-field term due to the electron-electron repulsion. When we study the dependence on the internuclear distance, we also make use of a 1D model of H_2^+ where the molecular axis is aligned with the polarization axis. In all cases, we work in the dipole approximation and in velocity gauge. In the 2D models, we take the electric field along the x axis, i.e., $\mathbf{E}(t)=(E(t),0,0)$. The two nuclei are placed at the positions (x_1,y_1) and (x_2,y_2) with $x_{1/2}=\pm R\cos\theta$ and $y_{1/2}=\pm R\sin\theta$, where θ is the angle between molecular axis and electric field. For H_2^+, the equilibrium internuclear distance is $R=2$ a.u., while for H_2 we have $R=1.4$ a.u. These are the values adopted in the calculation of the angle dependence but are varied to investigate the dependence on the internuclear distance.

The Hamiltonian for 2D H_2^+ is (in atomic units)

$$H=\frac{p_x^2}{2}+\frac{p_y^2}{2}+V(x,y)+p_xA(t), \tag{1}$$

where

$$V(x,y)=-\sum_{k=1,2}\frac{1}{\sqrt{(x-x_k)^2+(y-y_k)^2+\epsilon}} \tag{2}$$

and

$$A(t)=-\int_0^t E(t')dt'. \tag{3}$$

[The spatially constant term proportional to $A(t)^2$ has been eliminated by a unitary transformation.] In the soft-Coulomb potential, Eq. (2), the smoothing parameter ϵ was set to 0.5

*Present address: Instituto Nazionale Fisica della Materia–Dipartimento Scienze Fisiche, Via Cintia, 26-80126 Napoli, Italy.

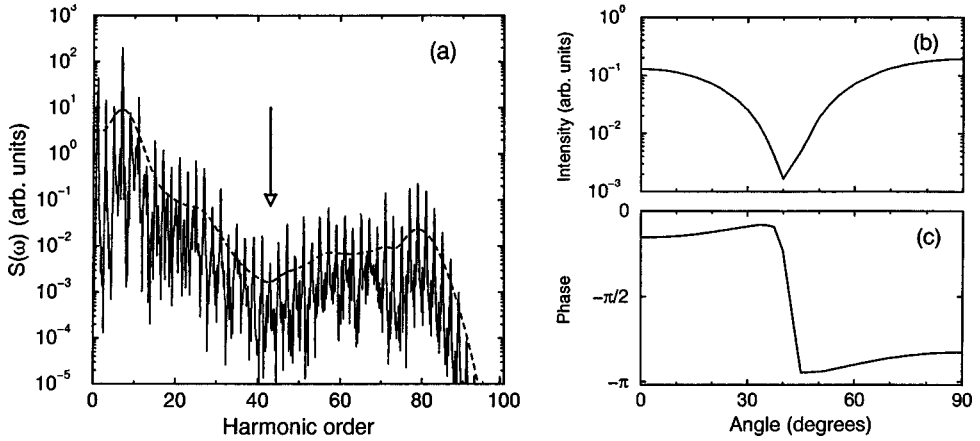

FIG. 1. (a) Harmonic spectrum for 2D H_2^+ in a laser pulse with intensity 5×10^{14} W/cm^2. The molecule is aligned at 40° relative to the polarization axis. Dashed line: smoothed spectrum. (b),(c) Orientation dependence of the harmonic intensity and phase for the 43rd harmonic.

so that the (purely electronic) H_2^+ ground-state energy of -30 eV is reproduced at $R=2$ a.u.

In the Hartree-Fock approximation for 2D H_2, the single-particle Hamiltonian has the same form as Eq. (1), but with the effective potential

$$V(x,y)=-\sum_{k=1,2}\frac{1}{\sqrt{(x-x_k)^2+(y-y_k)^2+\epsilon}}+\int\frac{|\psi(\tilde{x},\tilde{y},t)|^2 d\tilde{x}d\tilde{y}}{\sqrt{(x-\tilde{x})^2+(y-\tilde{y})^2+\eta}}. \quad (4)$$

Here, $\psi(x,y,t)$ is the time-dependent single-electron orbital. To reproduce the electronic ground-state energy and the ionization potential (-51 eV and 16 eV at $R=1.4$ a.u.), we choose smoothing parameters of $\epsilon=0.41$ and $\eta=0.36$.

The Hamiltonian for the 1D H_2^+ molecule is given by

$$H=\frac{p_x^2}{2}+V(x)+p_xA(t), \quad (5)$$

where

$$V(x)=-\sum_{k=1,2}\frac{1}{\sqrt{(x-x_k)^2+\epsilon}}. \quad (6)$$

Here, $\epsilon=1.44$ yields the correct electronic ground-state energy at $R=2$ a.u.

Unless stated otherwise, calculations have been performed for 780 nm trapezoidally shaped laser pulses with a total duration of 10 optical cycles and linear ramps of three optical cycles. The time evolution starts from the ground state which is obtained by propagation in imaginary time [20]. The time-dependent Schrödinger equation is solved by the split-operator method [21] with 2048 time steps per optical cycle.

The spectrum of emitted coherent radiation is obtained from time-dependent expectation values [22], either via calculating the time-dependent dipole moment or the time-dependent dipole acceleration. It was shown [23] that the spectrum is most precisely obtained from the dipole acceleration,

$$S_{\hat{\mathbf{e}}}(\omega)\sim|\hat{\mathbf{e}}\cdot\mathbf{a}(\omega)|^2=\left|\int\langle\psi(t)|\hat{\mathbf{e}}\cdot[\nabla V+\mathbf{E}(t)]|\psi(t)\rangle e^{i\omega t}dt\right|^2. \quad (7)$$

This is the spectrum of harmonics polarized along the direction of the unit vector $\hat{\mathbf{e}}$. In this paper, we take $\hat{\mathbf{e}}$ parallel to the laser polarization axis since the perpendicularly polarized harmonics are usually much weaker [18].

A typical numerical result is shown in Fig. 1(a) where we plot the spectrum of harmonics for the 2D H_2^+ molecule aligned at 40° relative to the polarization axis. A plateau with a cutoff at harmonic orders around 80 is clearly visible. The interesting feature of the spectrum is the pronounced minimum at the 43rd order. We have shown previously that destructive intramolecular interference is responsible for this minimum and that the frequency where the minimum is located increases when the angle of alignment is increased [18]. The width of this interference minimum is larger than the typical width of other structures in the spectral envelope. These other structures are due to interference between different electron trajectories [24]. To obtain a good estimate of the position of the minimum, we consider a smoothed spectrum where the fine structure has been eliminated by convolution with a Gaussian of appropriate width,

$$S_{\text{smooth}}(\omega)=\int S(\tilde{\omega})\exp(-(\tilde{\omega}-\omega)^2/\sigma^2)d\tilde{\omega}. \quad (8)$$

The smoothed spectrum in Fig. 1(a) (dashed line) was obtained with $\sigma=3\omega_L$, with ω_L being the frequency of the laser. We note that the minimum is indeed very close to the 43rd harmonic. After calculating the smoothed spectrum for various orientations of the molecule, we can plot the intensity of a particular harmonic order versus the angle θ as shown in Fig. 1(b) for the 43rd harmonic. We observe a minimum at a ''critical angle'' of 40°. This is a different perspective on exactly the same effect as seen in the spec-

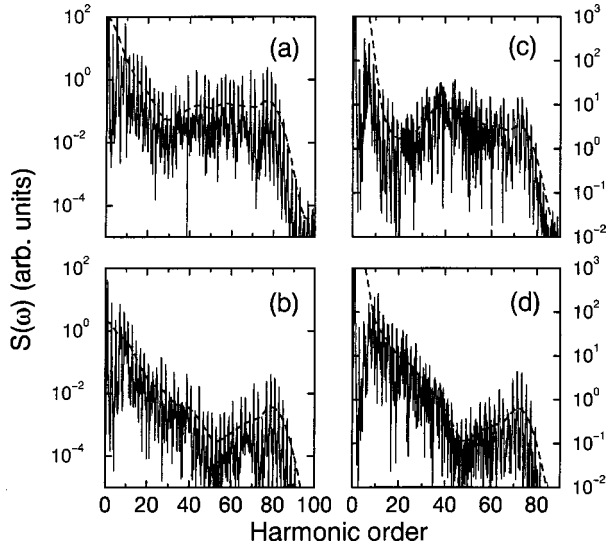

FIG. 2. Harmonic spectra for the 2D model molecules in a laser with intensity 5×10^{14} W/cm^2. Dashed curves: smoothed spectra. (a) H_2^+ at $\theta=40°$, $R=2.5$ a.u.; (b) H_2^+ at $\theta=40°$, $R=1.8$ a.u.; (c) H_2 at $\theta=0°$, $R=2.2$ a.u.; (d) H_2 at $\theta=0°$, $R=1.4$ a.u.

trum. Here, however, the position of the minimum can be localized more precisely. Figure 1(c) shows the typical behavior of the harmonic phase [18]: At the critical angle, there is a jump by almost π radians. Otherwise the phase depends only weakly on the angle. No smoothing has been employed to obtain the orientation dependence of the phase because it varies extremely rapidly with the harmonic frequency.

We proceed to investigate how the harmonic spectrum depends on the internuclear separation. In Figs. 2(a) and 2(b), we compare the spectra for 2D H_2^+ at $R=2.5$ a.u. and $R=1.8$ a.u. for an alignment angle of 40°. We may also compare with Fig. 1(a) showing the spectrum at the equilibrium separation $R=2$ a.u. It is evident that smaller internuclear distances lead to an interference minimum at a higher harmonic order. The same trend is found for 2D H_2 in Figs. 2(c) and 2(d), where we compare $R=2.2$ a.u. to the equilibrium distance $R=1.4$ a.u. at $\theta=0°$.

Before we present a systematic survey of how the position of the minimum depends on the geometry and orientation of the molecule, we briefly discuss what we should expect from simple physical arguments. In the recollision picture [5,6], HHG is understood as follows: First an electron is ejected from the molecule by tunnel ionization. Later this electron may recollide with the core and recombine so that a photon of high energy is emitted. Quantum mechanically, the recolliding electron is described by a wave packet, and its momentum p corresponds to a wavelength $\lambda=2\pi\hbar/p$. In the simplest model of this recollision, we consider a one-electron system being in a superposition of the ground state ψ_0 and a continuum wave packet ψ_c describing the recolliding electron:

$$\psi(\mathbf{r},t)=\alpha\psi_0(\mathbf{r},t)+\beta\psi_c(\mathbf{r},t). \tag{9}$$

The complex amplitude describing harmonic generation at the frequency ω is

$$A_{\hat{\mathbf{e}}}(\omega)=\int\langle\psi(t)|\hat{\mathbf{e}}\cdot[\boldsymbol{\nabla}V+\mathbf{E}(t)]|\psi(t)\rangle e^{i\omega t}dt. \tag{10}$$

The harmonics created in a single recollision event are obtained by inserting wave function (9) into Eq. (10). We ignore the contribution involving $\mathbf{E}(t)$ which gives nothing but the spectrum of the laser pulse. $A_{\hat{\mathbf{e}}}(\omega)$ then consists of several terms. The term describing transitions between the continuum and the ground state is given by

$$A_{\hat{\mathbf{e}},\mathrm{cg}}(\omega)=\alpha^*\beta\int\langle\psi_0(t)|\hat{\mathbf{e}}\cdot\boldsymbol{\nabla}V|\psi_c(t)\rangle e^{i\omega t}\,dt. \tag{11}$$

Our previous work [18] has shown that the intramolecular interference is essentially independent of the laser parameters and thus independent of how the electron is initially promoted into the continuum. Hence, we do not investigate how the electron is excited into the state ψ_c. Rather, we expect that the interference effect is explained by the structure of the recombination matrix element (11). For simplicity, consider a short-ranged potential well at each nucleus, i.e., $V(\mathbf{r})$ is zero except in regions around each nucleus, the diameters of which are small compared to the internuclear distance. Then, the matrix element in Eq. (11) is a sum of two terms,

$$A_{\hat{\mathbf{e}},\mathrm{cg}}(\omega)=A^{(1)}_{\hat{\mathbf{e}},\mathrm{cg}}(\omega)+A^{(2)}_{\hat{\mathbf{e}},\mathrm{cg}}(\omega), \tag{12}$$

each being an integral over a small region Ω_j around nucleus j located at $\mathbf{r}_j$. We further approximate the continuum wave function by a plane wave,

$$\psi_c(\mathbf{r},t)=e^{i\mathbf{k}\cdot\mathbf{r}-iE_{\mathbf{k}}t/\hbar}, \tag{13}$$

where $E_{\mathbf{k}}=\hbar^2k^2/2$ is the plane-wave energy. Taking the ground-state wave function to be constant inside the regions Ω_j and assuming that the continuum wave function varies no more than linearly within Ω_j leads to

$$A_{\hat{\mathbf{e}},\mathrm{cg}}(\omega)=-2\pi\hbar\,i\alpha^*\beta(\hat{\mathbf{e}}\cdot\mathbf{k})\,\delta(\hbar\omega-E_{\mathbf{k}}+E_0)\times\sum_j\psi_0(\mathbf{r}_j)e^{i\mathbf{k}\cdot\mathbf{r}_j}\int_{\Omega_j}V(\mathbf{r})d^nr. \tag{14}$$

Here, n is the dimensionality of the system. The δ function in Eq. (14) indicates that the frequency of the emitted radiation is given by the difference between the kinetic energy $E_{\mathbf{k}}$ of the recolliding electron and the ground-state energy $E_0=-I_\mathrm{p}$. (I_p is the ionization potential.) The factor $\hat{\mathbf{e}}\cdot\mathbf{k}$ expresses that the harmonics are polarized parallel to the direction of motion of the recolliding electron. Most interestingly, the term $\Sigma_j\psi_0(\mathbf{r}_j)\,e^{i\mathbf{k}\cdot\mathbf{r}_j}\int_{\Omega_j}V(\mathbf{r})d^nr$ describes the interference between the contributions from the various atomic centers. For homonuclear diatomic molecules, we have to sum over the two positions $\mathbf{r}_1$ and $\mathbf{r}_2=-\mathbf{r}_1$. The potential is symmetric, $V(\mathbf{r})=V(-\mathbf{r})$. Furthermore, for one- and two-electron systems, the ground-state orbital is symmetric, $\psi(\mathbf{r}_1)=\psi(\mathbf{r}_2)$, so that the relevant interference term is simply $e^{i\mathbf{k}\cdot\mathbf{r}_1}+e^{i\mathbf{k}\cdot\mathbf{r}_2}$. Destructive interference occurs when $\mathbf{k}$

$\cdot(\mathbf{r}_1-\mathbf{r}_2)=(2m+1)\pi/2$, or, in terms of the projected internuclear distance $R\cos\theta$ and the electron wavelength λ,

$$R\cos\theta=(2m+1)\lambda/2, \quad m=0,1,\ldots. \tag{15}$$

Constructive interference occurs for

$$R\cos\theta=m\lambda, \quad m=0,1,\ldots. \tag{16}$$

This result essentially describes the interference of two point emitters. It is far from obvious whether the same relations hold for real molecules at their equilibrium internuclear separations, because the Coulomb potential is long-ranged and the atomic wave functions strongly overlap. Nevertheless, Eqs. (15) and (16) explain why we have observed numerically only minima but no maxima so far: The first-order maximum [$m=1$ in Eq. (16)] is expected at half the wavelength of the first minimum [$m=0$ in Eq. (15)]. This corresponds to four times the harmonic order of the minimum and is typically in the frequency range beyond the cutoff, where the harmonic yield is very small. It is indeed possible to find maxima by looking at the orientation dependence of the harmonics at or beyond the cutoff.

Equation (14) implies that the wave vector of the recolliding electron is spatially constant and is determined by $E_{\mathbf{k}}=\hbar\omega+E_0=\hbar\omega-I_p$, where ω is the harmonic frequency. In an attractive long-ranged potential, however, the wavelength decreases when the electron enters the potential well around the nuclei. Within the potential well, we may still think of the wave function being approximately a plane wave, but with an effective wave vector determined by

$$E_{\mathbf{k}}=\hbar\omega. \tag{17}$$

Here we assume that the increase in the electron kinetic energy $E_{\mathbf{k}}$ upon entering the potential well is given by the ionization energy I_p on average. Whether this relation gives the wavelength that is physically relevant for the description of the intramolecular interference has to be investigated by inspection of the numerical results. In Fig. 3, we plot a collection of data points showing the relation between the projected internuclear distance $R\cos\theta$ and the wavelength λ of interference extrema. The wavelength is calculated via Eq. (17). The data were extracted from the numerical results in 2D, using smoothed versions of the harmonic spectra. Results are shown for H_2^+ and H_2 and for two different laser intensities. Both the internuclear distance and the molecular orientation have been varied. The lower set of points is for interference minima while the upper set of points is for interference maxima. In the latter case, only the higher laser intensity (10^{15} W/cm^2) was considered as it is just sufficient to have the interference maximum in the region around the cutoff. Also, at the higher intensity, only H_2^+ is studied because the H_2 molecule is ionized extremely rapidly. We find an almost linear relation between λ and $R\cos\theta$. In fact, the data points are surprisingly close to the dashed and dot-dashed lines, which show the predictions of Eq. (15) (with $m=0$) and Eq. (16) (with $m=1$). The wavelengths are systematically only slightly smaller than predicted by these simple formulas. The growing deviation for large wavelengths is probably due to the fact that these lower-order

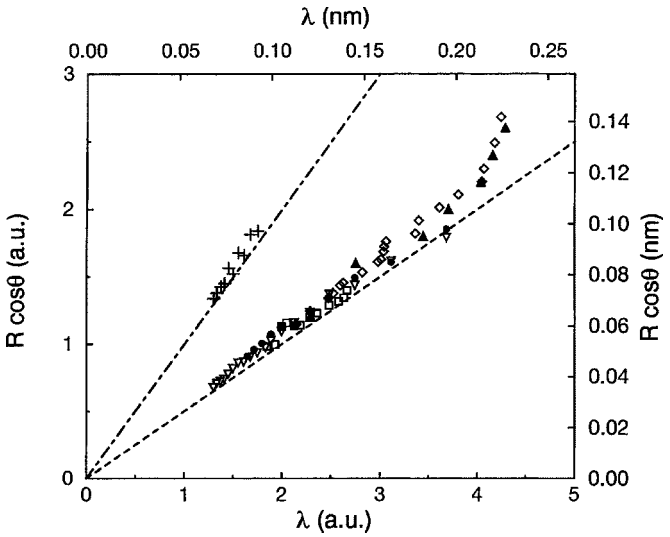

FIG. 3. Projected internuclear separation vs electron wavelength. Lower set of points: interference minima for the 2D model molecules. (∇) H_2^+ at $R=2$ a.u., $I=10^{15}$ W/cm^2, various θ; ($\bullet$) H_2^+ at $R=2$ a.u., $I=5\times10^{14}$ W/cm^2, various θ; ($\square$) H_2 at $R=1.4$ a.u., $I=5\times10^{14}$ W/cm^2, various θ; ($\diamond$) H_2^+ at $\theta=40°$, $I=5\times10^{14}$ W/cm^2, various R; ($\blacktriangle$) H_2 at $\theta=0°$, $I=5\times10^{14}$ W/cm^2, various R. Upper set of points ($+$): interference maxima for H_2^+ at $R=2$ a.u., $I=10^{15}$ W/cm^2, various θ.

harmonics involve recombination from low-energy continuum states or even excited bound states which are not well approximated by plane waves. Furthermore, harmonics of small frequency may also be generated by transitions from continuum states not into the ground state but into excited states, making the situation more complicated.

One of the main goals in HHG is the maximization of the harmonic yield. From this point of view, interference maxima are more interesting than minima. However, we have seen that maxima occur for rather large harmonic orders. A possibility to have maxima in the plateau region is to extend the plateau by increasing the laser intensity. Then, however, calculations in more than one dimension become very time-consuming. If the molecules are aligned parallel to the polarization axis, we may use the 1D model of H_2^+, Eqs. (5) and (6). We first show a comparison between 1D and 2D spectra in Fig. 4. The broad features of the two spectra are quite similar. For the lowest and highest harmonic orders (below 10 and above 70), even the fine structure looks almost identical. The interference minimum is not very deep but clearly visible at almost the same harmonic orders (25th order in 1D and 23rd order in 2D). We conclude that the intramolecular interference effects are not very sensitive to the dimensionality of the computation (if we are interested only in parallel alignment). The similarity between 1D and 2D results has been noted previously; see, e.g., Ref. [25].

For a laser intensity of 1.5×10^{15} W/cm^2, the plateau for H_2^+ extends up to about the 200th order. If we plot the intensity of the harmonics as a function of the internuclear distance, we find a clear interference pattern for harmonic orders close to the cutoff, see Fig. 5. The 195th harmonic exhibits two minima and two maxima in the range from $R=0$ to $R=3$ a.u. (not counting the one at $R=0$). For lower

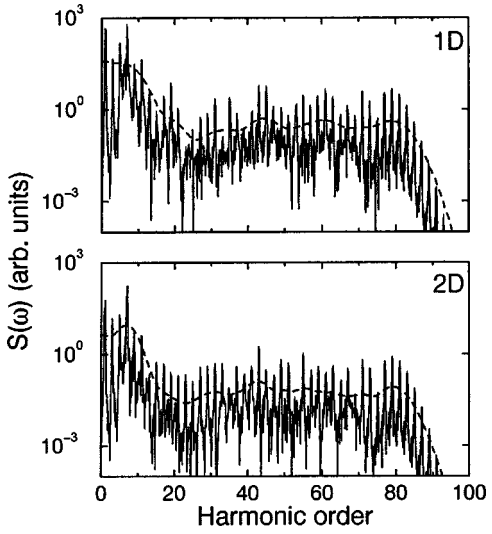

FIG. 4. Comparison between the harmonic spectra in 1D and 2D for H_2^+ aligned parallel to the laser polarization. The laser intensity is 5×10^{14} W/cm^2. Dashed curves: smoothed spectra.

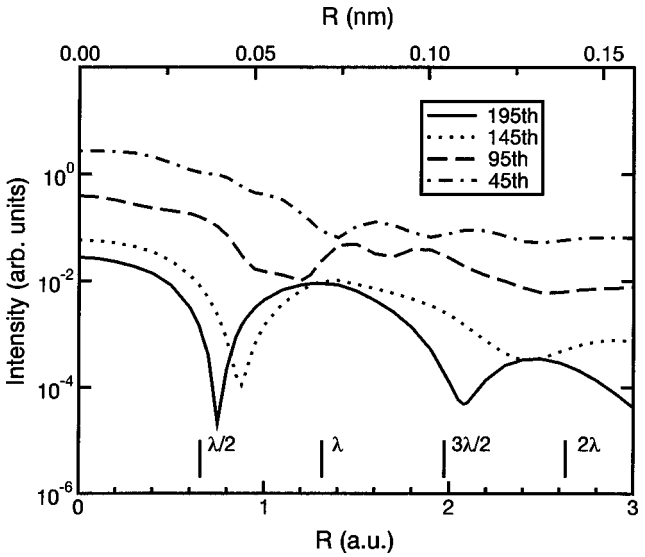

FIG. 5. Harmonic intensities vs internuclear distance R for 1D H_2^+ in a 10-cycle laser pulse with intensity 1.5×10^{15} W/cm^2 and two-cycle linear ramps. Harmonic orders are as indicated. The lines at the bottom mark the positions of destructive and constructive interference predicted by Eqs. (15) and (16) for the 195th harmonic.

harmonic orders, the interference pattern becomes less clear: While the first minimum remains intact, the structure at higher internuclear separations becomes irregular and relatively flat. A possible reason is that HHG at lower orders is complicated by transitions into excited states as explained above. For the 195th harmonic, the marks at the bottom of the figure indicate the positions where perfect destructive or constructive interference is expected according to Eqs. (15) and (16), with the wavelength calculated from Eq. (17). Except for the last maximum, we find very good agreement with the numerical results. The clear appearance of the interference maxima at not too large bond lengths suggests that these maxima may well be observed experimentally if an appropriate molecular species is chosen. Furthermore, as a molecule dissociates, it will inevitably pass through a maximum with increasing internuclear separation.

It was found that for large bond lengths the cutoff moves to higher frequencies in the harmonic spectrum [10,11]. These high-order harmonics are due to electrons that emerge at one atomic center and recombine at a different atomic center. Although a wider range of harmonics thus becomes observable, it is unlikely that this effect reveals more of the interference structure, because the latter is due to electrons recolliding with the molecular core as a whole rather than a single atomic site.

We note that the interference pattern depends crucially on the symmetry of the molecular valence orbital: If an odd wave function ψ_0 appears in Eq. (14), then the conditions for constructive or destructive interference will be interchanged. Thus, molecules with odd valence orbitals should exhibit maxima at lower harmonic orders, which makes them easier to be found in experiment. The O_2 molecule is a particularly promising candidate because previous work strongly suggests that that the ionization probability of O_2 is reduced by intramolecular interference [26–29].

To summarize, we have investigated HHG in small molecules. The harmonic spectra as well as their dependence on the molecular orientation and internuclear distance contain interference patterns that are due to interfering contributions emitted from the different atomic centers. In many cases, the interference pattern is correctly predicted by a simple picture regarding the nuclei as point emitters. Like dynamic electron diffraction, the effect may thus be interpreted as microscopic two-slit interference with the difference being that in HHG, the incident wave (electron) and the generated wave (photons) are not the same kind of wave. Two main experimental applications may be envisaged. First, specific harmonics can be maximized by using configurations where constructive interference is realized. This will be achieved by choosing appropriate molecules and applying alignment techniques. Second, information about the molecular structure can be obtained from the harmonic spectra. Hence, they may serve as a probe of nuclear dynamics.

We gratefully acknowledge discussions with Paul Corkum and Misha Ivanov. This work was supported by the UK Engineering and Physical Sciences Research Council and by the European Union IHP Program (HPMF-CT-1999-00346 and HPRN-CT-1999-00129).

[1] A. McPherson *et al.*, J. Opt. Soc. Am. B **4**, 595 (1987).
[2] A. L'Huillier, K.J. Schafer, and K.C. Kulander, J. Phys. B **24**, 3315 (1991).
[3] M. Protopapas, C.H. Keitel, and P.L. Knight, Rep. Prog. Phys. **60**, 389 (1997).
[4] P. Salières, A. L'Huillier, P. Antoine, and M. Lewenstein, Adv. At., Mol., Opt. Phys. **41**, 83 (1999).
[5] P.B. Corkum, Phys. Rev. Lett. **71**, 1994 (1993).

[6] K.C. Kulander, J. Cooper, and K.J. Schafer, Phys. Rev. A **51**, 561 (1995).
[7] M.Yu. Ivanov and P.B. Corkum, Phys. Rev. A **48**, 580 (1993).
[8] T. Zuo, S. Chelkowski, and A.D. Bandrauk, Phys. Rev. A **48**, 3837 (1993).
[9] H. Yu and A.D. Bandrauk, J. Chem. Phys. **102**, 1257 (1995).
[10] P. Moreno, L. Plaja, and L. Roso, Phys. Rev. A **55**, R1593 (1997).
[11] R. Kopold, W. Becker, and M. Kleber, Phys. Rev. A **58**, 4022 (1998).
[12] D.G. Lappas and J.P. Marangos, J. Phys. B **33**, 4679 (2000).
[13] O.E. Alon, V. Averbukh, and N. Moiseyev, Phys. Rev. Lett. **80**, 3743 (1998); V. Averbukh, O.E. Alon, and N. Moiseyev, Phys. Rev. A **64**, 033411 (2001).
[14] A.D. Bandrauk and H. Yu, Phys. Rev. A **59**, 539 (1999).
[15] T. Kreibich, M. Lein, V. Engel, and E.K.U. Gross, Phys. Rev. Lett. **87**, 103901 (2001).
[16] R. Velotta, N. Hay, M.B. Mason, M. Castillejo, and J.P. Marangos, Phys. Rev. Lett. **87**, 183901 (2001).
[17] N. Hay *et al.*, Phys. Rev. A **65**, 053805 (2002).
[18] M. Lein, N. Hay, R. Velotta, J.P. Marangos, and P.L. Knight, Phys. Rev. Lett. **88**, 183903 (2002).
[19] P. Corkum and M. Ivanov (private communication); H. Niikura *et al.*, Nature (London) **417**, 917 (2002).
[20] R. Kosloff and H. Tal-Ezer, Chem. Phys. Lett. **127**, 223 (1986).
[21] M.D. Feit, J.A. Fleck, Jr., and A. Steiger, J. Comput. Phys. **47**, 412 (1982).
[22] B. Sundaram and P.W. Milonni, Phys. Rev. A **41**, 6571 (1990); J.H. Eberly and M.V. Fedorov, *ibid.* **45**, 4706 (1992); D.G. Lappas, M.V. Fedorov, and J.H. Eberly, *ibid.* **47**, 1327 (1993).
[23] K. Burnett, V.C. Reed, J. Cooper, and P.L. Knight, Phys. Rev. A **45**, 3347 (1992).
[24] M. Lewenstein, Ph. Balcou, M.Yu. Ivanov, A. L'Huillier, and P.B. Corkum, Phys. Rev. A **49**, 2117 (1994).
[25] R.M. Potvliege, N.J. Kylstra, and C.J. Joachain, J. Phys. B **33**, L743 (2000).
[26] A. Talebpour, C.-Y. Chien, and S.L. Chin, J. Phys. B **29**, L677 (1996).
[27] C. Guo, M. Li, J.P. Nibarger, and G.N. Gibson, Phys. Rev. A **58**, R4271 (1998).
[28] C. Guo, Phys. Rev. Lett. **85**, 2276 (2000).
[29] J. Muth-Böhm, A. Becker, and F.H.M. Faisal, Phys. Rev. Lett. **85**, 2280 (2000).